A Control Strategy for a Robot with One Articulated Leg Hopping on Irregular Terrain

J. Vermeulen, D. Lefeber & H. De Man

Vrije Universiteit Brussel, Department of Mechanical engineering, Pleinlaan 2, 1050 Brussels, Belgium
Jimmy Vermeulen: tel: +32-2-629.28.08, fax: +32-2-629-28-65, e-mail: Jimmy.Vermeulen@vub.ac.be

abstract

This paper reports on an improvement of an earlier developed control algorithm for a one-legged hopping robot. The algorithm, which allows the robot to hop on irregular terrain, consists of two separate parts. By steering the motion of the leg the first part controls a number of objective locomotion parameters, being forward velocity during flight, hopping height, step length and stepping height. These objective parameters can be changed from one hop to another. This part of the algorithm has been extensively discussed in [3]. The second part of the algorithm controls the motion of the upper body, by making an adequate choice of the angular momentum around the COG during the flight phase and by choosing a well determined value of the stance time. This paper specifically focuses on the control of the upper body motion. Although the algorithm allows for non-steady state motion, for simplicity reasons the control of the upper body will first be tested on a number of consecutive steady state hops.

1. INTRODUCTION

When compared to the various publications made on walking machines, few research has been done on running robots. Although the control of running robots is more complex, motion can be much more performant. Because of the existence of ballistic flight phases, a running machine can attain higher forward velocities and can take steps with a greater length and a greater height. The best known running robots are of course the ones developed by Raibert's team at the MIT [5]. However, the control algorithm used by these machines was basically a steady state algorithm and has little control on the placement of the foot on possible footholds, making its usefulness for locomotion on irregular terrain quite limited [4].

At the Department of Mechanical Engineering of the Vrije Universiteit Brussel, research has been focused on the latter group of machines. The model being recently under study is a one-legged hopping robot with an articulated leg, designed for hopping on unstructured terrain. Earlier, De Man et al. introduced a control algorithm, which was first applied to a model with a telescopic leg [1], and later to a model with an articulated leg [2], [3] and [6]. This algorithm makes it possible to place the robot's foot exactly on a desired foothold and to control its forward velocity during flight. Further research on an experimental prototype showed however that the algorithm had some drawbacks concerning the behaviour of the upper body. The aim of this paper is to overcome these drawbacks, which results in a more effective algorithm.

In section 2 of the paper a description of the model is given. Section 3 explains the underlying idea of the control algorithm. In section 4 simulation results are given, whereas in section 5 conclusions are drawn.

2. THE MODEL [3]

The control of a running machine is more critical than the control of a walking machine. To be able to study all the features of a running machine, such as its underactuated and nonholonomic nature, without unnecessarily increasing the complexity of its design, a robot having one articulated leg is considered here and its motion is restricted to the sagittal plane.

Figure 1 depicts the robot at the moment of take-off and at the moment of touch-down. The robot consists of three segments: a lower leg (segment 1), an upper leg (segment 2) and a body (segment 3). The different links are connected to each other through rotational uni-axial joints.

The length of the i-th link is l_i, its mass is m_i and the moment of inertia around its center of mass G_i is I_i. The angle between the horizontal and the i-th segment is θ_i. Point F will further be referred to as the foot of the robot, point K as its knee and point H as its hip. The location of the center of mass G_1 of the lower leg and the location of the center of mass G_2 of the upper leg are given by $FG_1 = \alpha l_1$ and $KG_2 = \beta l_2$, where $0 < \alpha, \beta < 1$. The center of mass G_3 of the body coincides with the hip.

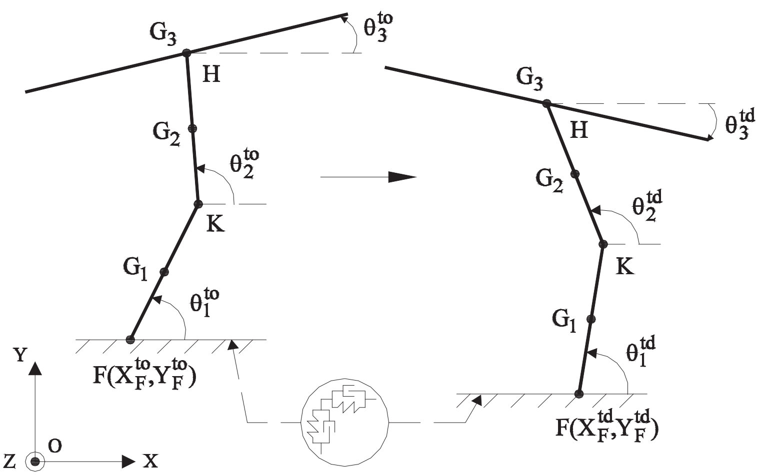

Figure 1: robot at take-off (to) and at touch-down (td)

The actuation of the robot consists of a passive part, formed by a torsional spring placed at the knee, and an active part, built up by two actuators exerting a torque at the knee and a torque at the hip respectively. For the sake of clarity the spring and the actuators are not depicted on the figure.

The ground is modelled as a spring-damper combination. Both in the horizontal and in the vertical direction a stiff linear spring and a damper are placed in parallel. This model allows to simulate the flight phase, during which there is no contact with the ground, the impact phase, when the foot hits the ground, and the stance phase, during which the robot stands on the ground, all without mathematically changing the number of degrees of freedom (DOF) of the system. However, by tuning the spring constants and the damping coefficients it is possible to keep the displacement of the foot during stance arbitrarily small, thus virtually reducing the number of DOF of the robot.

Considering the previous remark the robot has 5 DOF during flight and 3 DOF during stance (the assumption has been made that the foot of the robot does not slip). The generalized coordinates used to describe the motion of the robot are the coordinates X_F and Y_F of the foot, measured in the reference frame OXYZ, and the angles θ_1, θ_2 and θ_3.

3. THE CONTROL ALGORITHM

3.1 Flight Phase

3.1.1 Leg Motion [3]

Since the center of gravity of the body coincides with the hip, the orientation of the body has no influence on the position of the global center of mass. This means that there is a complete decoupling between the motion of body and leg. The motion of the leg determines the motion of the center of mass. Constraining the motion of the center of gravity to a ballistic trajectory results in 2 constraint equations on the 4 generalized coordinates $(X_F,\, Y_F,\, \theta_1,\, \theta_2)$ of the leg, which means that only two of these coordinates are independently controllable.

The two controlled coordinates being chosen in this paper are the absolute angles of lower and upper leg with respect to the horizontal axis, being θ_1 and θ_2.

Relationships between the equations dictating the parabolic trajectory of the global center of gravity and the objective locomotion parameters to be controlled, being the forward velocity, the jumping height and the position of the foot at touch-down, are established [3]. Using these relationships the orientation θ_1 of the lower leg, the orientation θ_2 of the upper leg, the angular velocities $\dot{\theta}_1$ and $\dot{\theta}_2$, and the angular accelerations $\ddot{\theta}_1$ and $\ddot{\theta}_2$, needed at take-off and touch-down are calculated. Next, reference trajectories for both angles, being noted as $\theta_1(t)^{fl}$ and $\theta_2(t)^{fl}$ are generated, satisfying the boundary conditions at take-off and touch-down. These trajectories are 5th order polynomial functions, being tracked by the PD-controlled actuators at knee and hip respectively.

3.1.2 Body Motion

The only generalized coordinate associated with the upper body motion, being its absolute angle with respect to the horizontal axis θ_3, is submitted to the nonholonomic angular momentum constraint with respect to the global center of gravity. Thus, body attitude can not be directly controlled during flight, its pitch angle and angular rate are determined by inertia. In this model, body inertia is chosen significantly larger than leg inertia, in order to reduce the upper body rotation resulting from the leg swing during flight.

During flight the angular momentum with respect to the global COG equals a constant. It can be written as follows:

$$\mu_G^{fl}(t) = c\dot{\theta}_1 + d\dot{\theta}_2 + e(\dot{\theta}_1 + \dot{\theta}_2)\cos(\theta_1 - \theta_2) + f\dot{\theta}_3 = \mu_G^{fl} \tag{1}$$

The constants c, d, e, and f are determined by the lengths and mass and inertia parameters of the different links.

Integrating (1) from 0 to the flight time T^{fl} leads to the following expression for the upper body rotation during flight:

$$\Delta\theta_3^{fl} = \frac{\mu_G^{fl} T^{fl} - A^{fl}}{f} \tag{2}$$

with:

$$A^{fl} = c\Delta\theta_1^{fl} + d\Delta\theta_2^{fl} + e\int_0^{T^{Fl}} (\dot{\theta}_1 + \dot{\theta}_2)\cos(\theta_1 - \theta_2)\, dt \tag{3}$$

and $\Delta\theta_i^{fl}$ representing the variation of θ_i during flight.

It is clear, that if we want to control the motion of the upper body, the rotation given in (2) should be compensated during the stance phase. If not, the rotation starts drifting which eventually causes the robot to fall.

3.2 Stance Phase

3.2.1 Leg Motion [3]

Because of the constraint on the leg during stance demanding that the foot should stay at a fixed position, the same two controlled coordinates are chosen as during flight. Let's consider a hopping pattern of steady-state consecutive hops as a first experiment. For the robot to be able to perform a hop with certain desired values for the objective locomotion parameters, there is some control needed during the stance phase, yielding the desired initial conditions at take-off. Thus, the values for θ_1, θ_2, and their first and second derivatives at the end of the stance phase are those of the beginning of the next flight phase. The values for θ_1, θ_2, and their first and second derivatives at the beginning of the stance phase are those measured after impact.

Again, in an analogue way as during flight, 5th order polynomials can be calculated, which are the reference trajectories $\theta_1(t)^{st}$ and $\theta_2(t)^{st}$ for lower and upper leg respectively, being tracked by the PD-controlled acuators at knee and hip.

3.2.2 Body Motion

During stance, body motion is submitted to a constraint, resulting from the fact that the angular momentum with respect to the foot only depends on gravity. The rotation of the upper body is determined by this constraint and can therefore not directly be controlled. However, by making a good choice of the angular momentum with respect to the COG during flight and the stance time, the robot will be able to compensate the rotation of the body caused during the preceding flight phase.

During stance a rotation of the body $\Delta\theta_3^{st}$ is introduced. We reach a controlled body motion when, considering one flight and stance phase, following condition is achieved:

$$\Delta\theta_3^{fl} + \Delta\theta_3^{st} = 0 \tag{4}$$

Integration of angular momentum constraint with respect to the footpoint F yields the variation of the angular momentum during stance:

$$\Delta\mu_F^{st} = -gM \int_0^{T^{st}} (a\cos\theta_1 + b\cos\theta_2)\,dt \tag{5}$$

Where a and b are constants determined by the lengths and masses of lower and upper leg.

Since we consider steady-state motion, the angular momentum with respect to G in the next flight phase should be equal to the one in the preceding flight phase. By making use of this condition and by applying the transport equation on the angular momentum, the left hand side of (5) is completely determined. This means that (5) determines an ideal value for the stance time T^{st*}, which guarantees that the angular momentum with respect to the COG will be the same in the two consecutive flight phases.

Further, it can be shown that $\Delta\theta_3^{st}$ is given by:

$$\Delta\theta_3^{st} = \frac{(\mu_G^{fl} + B^{st})T^{st*} - A^{st}}{s} \tag{6}$$

with:

$$\begin{aligned} A^{st} = p\Delta\theta_1^{st} + q\Delta\theta_2^{st} + r \int_0^{T^{st*}} (\dot{\theta}_1 + \dot{\theta}_2)\cos(\theta_1 - \theta_2)\,dt \\ + gM \int_0^{T^{st*}} \left(\int_0^{\epsilon} (a\cos\theta_1 + b\cos\theta_2)\,d\epsilon\right) dt \end{aligned} \tag{7}$$

and:

$$B^{st} = \Delta\mu_F^{shock} + (\bar{FG}^{td} \times M\bar{V_G}^{td})|_z \tag{8}$$

The constants p, q, r and s are determined by the lengths and mass and inertia parameters of the different links. M is the total mass of the robot and $\Delta\mu_F^{shock}$ is the variation of μ_F during impact.

Imposing (4), leads then to a linear equation which can be solved for μ_G^{fl}, resulting in a desired value for the angular momentum with respect to G during flight μ_G^{fl*}:

$$\mu_G^{fl*} = \frac{A^{fl} + A^{st} - B^{st}T^{st*}}{T^{fl} + T^{st*}} \tag{9}$$

which can of course be translated in a desired value for $\dot{\theta_3}^{to}$. Thus, when the robot starts its first flight phase with the right angular velocity of the body , and when the actuators track the desired polynomials during flight and stance respectively, the robot reaches steady state motion. This steady state behaviour guarantees the same values for the objective locomotion parameters during the consecutive hops, as well as a stabilized motion of the body.

4. SIMULATION RESULTS

To test the algorithm described above a hopping pattern consisting of a number of consecutive hops has been simulated. Since we consider steady state behaviour, the values of the desired objectives, being forward velocity during flight, step length, stepping height, orientation of the leg at take-off and touch-down, and behaviour of the body, are the same for all hops. The chosen parameters are the following:

- $\dot{X_G}^* = 1$ m/s
- $X_F{}^* = 0.5$ m
- $Y_F{}^* = 0$ m
- $\theta_3^{to} = 0$

This results in:

- $\mu_G^{fl*} = 0.622\ kgm^2/s$
- $\Delta\theta_3^{fl} = 0.1084$ rad $= -\Delta\theta_3^{st}$
- $T^{st*} = 0.34$ s

Figure 2 shows the rotation of the upper body θ_3 versus time. The graph shows that the rotation during stance is equal and opposite to the rotation during flight. Thus, after one stride, the angle equals zero again.

Figure 3 gives the angular momentum μ_G with respect to G versus time. The horizontal parts of the graph give the momentum during the flight phase, equaling the ideal value as calculated by the control algorithm.

Figure 4 shows the horizontal position X_F of the foot point F versus time. The horizontal parts of the graph give the position of the foot during the successive stance phases. It can be seen that the difference between the position during two successive stance phases is equal to the desired step length of 0.5 m.

Figure 5 shows the forward velocity $\dot{X}_G$ of the global center of mass versus time. The horizontal parts of the graph give the velocity during the flight phase, equaling the desired value of 1 m/s.

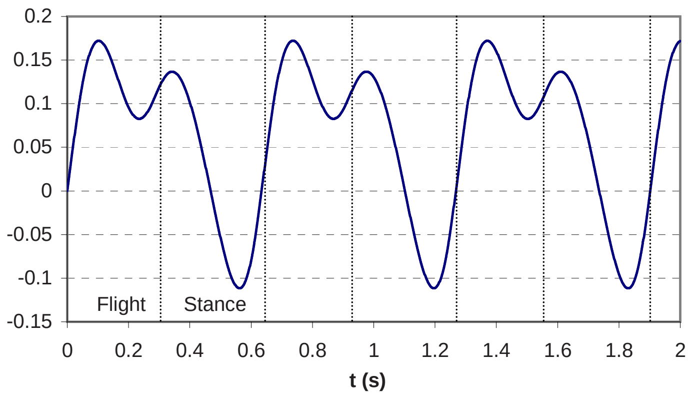

Figure 2: θ_3 $[rad]$ as a function of time

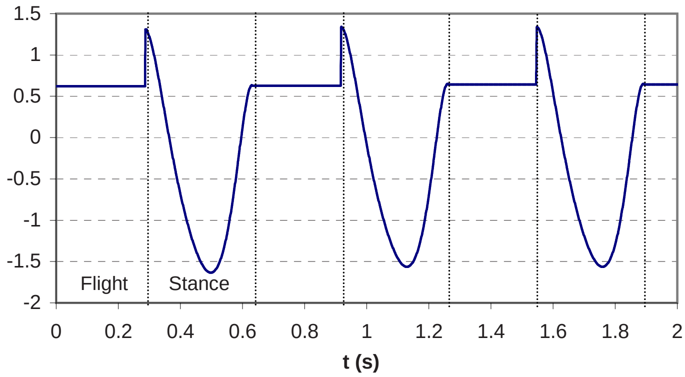

Figure 3: μ_G $[kgm^2/s]$ as a function of time

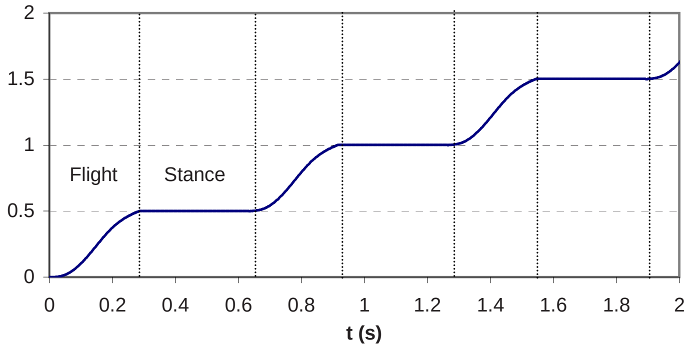

Figure 4: X_F $[m]$ as a function of time

5. CONCLUSIONS

A control algorithm for a one-legged hopping robot has been developed. The algorithm allows to change a number of objective locomotion parameters from one hop to another. During this motion, the upper body behaviour has to be controlled. Simulations show that in the case of a steady-state motion, the body motion can be controlled without introducing extra torques directly acting on the body. By making a specific choice of the angular momentum during flight

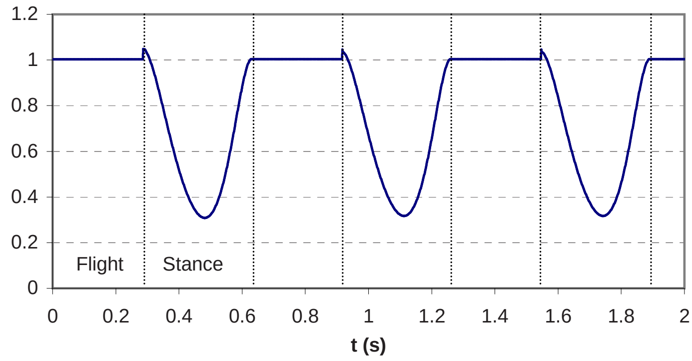

Figure 5: $\dot{X}_G$ $[m/s]$ as a function of time

and by choosing a well determined value of the stance time, the rotation of the upper body caused in a preceding flight phase is automatically compensated in the next flight phase. For the moment, simulations are being performed where transitions from one steady state motion to another are made.

References

[1] H. De Man, D. Lefeber, F. Daerden, and E. Faignet. Simulation of a New Control Algorithm for a One-Legged Hopping Robot (Using the Multibody Code Mechanica Motion). In *Proceedings International Workshop on Advanced Robotics and Intelligent Machines*, Manchester, United Kingdom, 1996.

[2] H. De Man, D. Lefeber, and J. Vermeulen. Control on Irregular Terrain of a Hopping Robot with One Articulated Leg. In *Proceedings of the 8th International Conference on Advanced Robotics: Workshop II: New Approaches on Dynamic Walking and Climbing Machines*, pages 72–76, Monterey, California, USA, 1997.

[3] H. De Man, D. Lefeber, and J. Vermeulen. Design and Control of a One-Legged Robot Hopping on Irregular Terrain. In *Proceedings Euromech 375: Biology and Technology of Walking*, pages 173–180, Munich, Germany, 1998.

[4] J.K. Hodgins. *Legged Robots on Rough Terrain: Experiments in Adjusting Step Length*. PhD thesis, Carnegie Mellon University, November 1989.

[5] M.H. Raibert. *Legged Robots that Balance*. MIT Press, Cambridge, Massachusetts, 1986.

[6] Z. Terze, D. Lefeber, J. Vermeulen, and H. De Man. Setting Objective Parameters of a Hopping Robot Based on Power Consumption. In *Proceedings CLAWAR98: First International Symposium on Mobile, Climbing and Walking Robots*, pages 297–302, Brussels, Belgium, 1998.